IMPACTS OF URBANIZATION AND CLIMATE CHANGE OVER THE 21ST CENTURY ON COASTAL WIND RESOURCES IN THE MID-ATLANTIC U.S.

by

Brian P. Frei

A thesis submitted to the Faculty of the University of Delaware in partial fulfillment of the requirements for the degree of Master of Science in Geography

Summer 2022

IMPACTS OF URBANIZATION AND CLIMATE CHANGE OVER THE 21ST CENTURY ON COASTAL WIND RESOURCES IN THE MID-ATLANTIC U.S.

by

Brian P. Frei

Approved: _____

Dana E. Veron, Ph.D.
Co-advisor in charge of thesis on behalf of the thesis Advisory Committee

Approved: _____

Jing Gao, Ph.D.
Co-advisor in charge of thesis on behalf of the thesis Advisory Committee

Approved: _____

Saleem Ali, Ph.D.
Chair of the Department of Geography & Spatial Sciences

Approved: _____

Fabrice Veron, Ph.D.
Dean of the College of Earth, Ocean & Environment

Approved: _____

Louis F. Rossi, Ph.D.
Vice Provost for Graduate and Professional Education and
Dean of the Graduate College

ACKNOWLEDGMENTS

Dr. Dana Veron and Dr. Jing Gao, for their support and guidance over the last two years.

Dr. Stefan Rahimi, for his assistance on the regional climate model configuration.

Dr. Melissa Bukovsky, for her help integrating urban land use changes into the model simulations.

Eric Allen, for his advice and technical support on model physics.

Dr. Joseph Brodie, for introducing me to the excitement of atmospheric research and mentoring me throughout my academic career.

NCAR's Computational Information System Laboratory, for the data access and computing support provided by the NCAR CMIP Analysis Platform (doi:10.5065/D60R9MSP) and the high-performance computing support on Cheyenne (doi:10.5065/D6RX99HX).

This manuscript is dedicated to

My parents and brother for supporting me throughout my life and giving me the opportunity to pursue my dreams.

My friends and girlfriend for always being there for me through the ups and downs.

All of my mentors who helped me build the skills necessary to pursue this project.

TABLE OF CONTENTS

LIST OF FIGURES

LIST OF TABLES

ABSTRACT

Climate change and urbanization can alter coastal wind resources available for energy production by modifying pressure patterns, local thermodynamics, and land surface properties. The Mid-Atlantic U.S. has a burgeoning offshore wind industry, with strong potentials for drastic climate change and widespread urbanization. Here I investigate how climate change and urbanization over the 21st century collectively and respectively affect coastal winds, using the Mid-Atlantic U.S. as an example region. Urbanization causes increased summertime wind speeds over the ocean (0.4 – 0.6 m/s) and decreased wind speeds over land with minimal offshore impacts in other seasons. Similarly, climate change causes the largest impacts on wind resources in the summer, with offshore wind speed increases between 0.8 – 1.4 m/s. While urbanization strengthens the sea breeze circulation through enhanced land-ocean temperature gradients, climate change weakens it. Both climate change and urbanization cause substantial increases in extreme heat conditions in the Mid-Atlantic U.S. These findings suggest that the impacts of both urbanization and climate change are vital to consider as offshore wind energy develops along urbanizing coastal areas.

Chapter 1

INTRODUCTION

Offshore wind energy is a rapidly developing form of renewable energy, growing 30% globally between 2010 and 2018 (Wind Outlook, 2019). As this market expands, it is important to understand how climate change and land use change such as urbanization can impact offshore wind resources. Existing studies that simulate the impacts of climate change on wind speeds exhibit contradictory results and contain large uncertainties (Wu et al., 2020, Craig et al., 2019). The impacts of historical urbanization have been considered in several studies (Chen et al., 2020, Hou et al., 2013), however, the effects of future urbanization on wind resources have not been studied. Here I investigate the impacts of 21st century urbanization and climate change on regional climate conditions, especially wind resources, using high-resolution regional climate modeling in the Mid-Atlantic U.S. due to the region's rapidly developing offshore wind industry and potential for drastic climate change as well as widespread urbanization (Gao et al., 2020).

Most studies investigating the impacts of climate change on wind speeds focus on global or continental scales using regional and global climate models (GCMs and RCMs)

(Martinez and Iglesias, 2022, Vu Dinh et al., 2022, Costoya et al., 2020, Pryor et al., 2020, Chen, 2020, Sawadogo et al., 2020, Craig et al., 2019, Reboita et al., 2018, Davy et al., 2018, Karnauskas et al., 2018, Carvalho et al., 2017, Haupt et al., 2016, Johnson and Erhardt, 2016) and there are limited regional climate simulations at convection-permitting resolution (<4km). While there is still considerable uncertainty among projections, several studies find decreasing winds in the eastern U.S. as a result of future climate change (Martinez and Iglesias, 2022, Costoya et al., 2020, Pryor et al., 2020, Johnson and Erhardt, 2016). This is consistent with global and northern hemisphere decreases in historical surface wind speeds (Wu et al., 2020, Zhang et al., 2019), although one study (Zeng et al., 2019) finds a reversal to increasing wind speeds beginning in 2010 and attributes much of the historical wind speed changes to decadal-scale patterns in the ocean and atmosphere. One simulation focused on temperature and precipitation in the Northeastern U.S. finds substantial value added through convection-permitting regional climate modeling (Komurcu, 2018). In the coastal Mid-Atlantic, mesoscale phenomena such as the sea breeze circulation are an important source of variability in the wind field (Xia et al., 2022, McCabe, 2021, Seroka et al., 2018, Hughes and Veron, 2015, Bowers, 2004), particularly during the summer months when energy demands are high and average wind speeds are at an annual minimum (Veron et al., 2018). Therefore, I employ convection-permitting RCMs at 3-km resolution to investigate the local impacts of climate change on coastal wind patterns in the Mid-Atlantic.

Furthermore, urbanization is necessary to consider because of its impacts on surface roughness, heat, and moisture transfer which influence local and regional dynamics. Urban land in the coastal Mid-Atlantic U.S. can expand substantially over the 21st century under the Shared Socioeconomic Pathway 5 (SSP5, a fossil-fueled development scenario) (Gao & O'Neill, 2020, Kriegler et al., 2017) . Land-use changes are known to alter climate conditions (Bukovsky et al., 2021, Chen et al., 2020, Zhang et al., 2019, Yan et al., 2016, Wu et al., 2016, Hou et al., 2013, Kalnay and Cai, 2003) and have been shown to impact sea breeze circulations (Varquez et al., 2014, Chen et al., 2011, Childs and Raman 2005); however, little is known about how future urbanization may affect coastal winds. Additionally, while urbanization is known to cause slower wind speeds within cities (Chen et al., 2020, Yan et al., 2016, Hou et al., 2013) and has been found to impact precipitation and temperature in areas surrounding cities (Bukovsky et al., 2021, Daniel et al., 2019), the regional impacts of urbanization on winds in surrounding areas are not well studied. At the end of the 21st century, urban areas across the world are expected to experience up to 4 ℃ warmer temperatures than their surrounding areas (Zhao et al., 2021) and urban expansion has been linked to increased risks of heat-related illness (Chen et al., 2010). The sea breeze circulation serves an important role in temperature moderation of coastal populations by transporting cooler ocean air onshore (Zhou et al., 2019). Therefore, in addition to climate change impacts it is imperative to consider the effects of future urbanization on coastal winds.

Addressing these gaps in literature, I develop a high-resolution two-domain (15 km, 3km resolution) RCM configuration (Fig. 1) to investigate the separate and combined effects of climate change and urbanization at the end of the 21st century on wind resources in the Mid-Atlantic U.S. I use the Weather Research and Forecasting (WRF) model as an RCM with climate boundary conditions from the Community Earth System Model Version 2 (CESM2) (Danabasoglu et al., 2020) and integrate spatially-explicit urban land change over the 21st century from a state-of-the-art SSP-consistent spatial urban land dataset (Gao and Pesaresi 2021, Gao and O'Neill 2020). Climate boundary conditions at the end of the century are based on Representative Concentration Pathway 8.5 (RCP8.5, an average carbon forcing of 8.5 W/m2) (Riahi et al., 2011), which pairs consistently with SSP5 in the Scenario Model Intercomparison Project (ScenarioMIP) (O'Neill et al., 2016). I examine four 10-year scenarios: historical urban land extent and climate conditions (2005 – 2015) (HIST_HIST), SSP5 urban land extent in 2100 and historical climate conditions (SSP5_HIST), historical urban land extent and EOC RCP8.5 climate conditions (HIST_RCP8.5) (2090 – 2099), and urban and extent in 2100 and EOC RCP8.5 climate conditions (SSP5_RCP8.5). Urbanization (SSP5_HIST – HIST_HIST), climate change (HIST_RCP8.5 – HIST_HIST), and combined (SSP5_RCP8.5 – HIST_HIST) impacts are discussed in the following results sections.

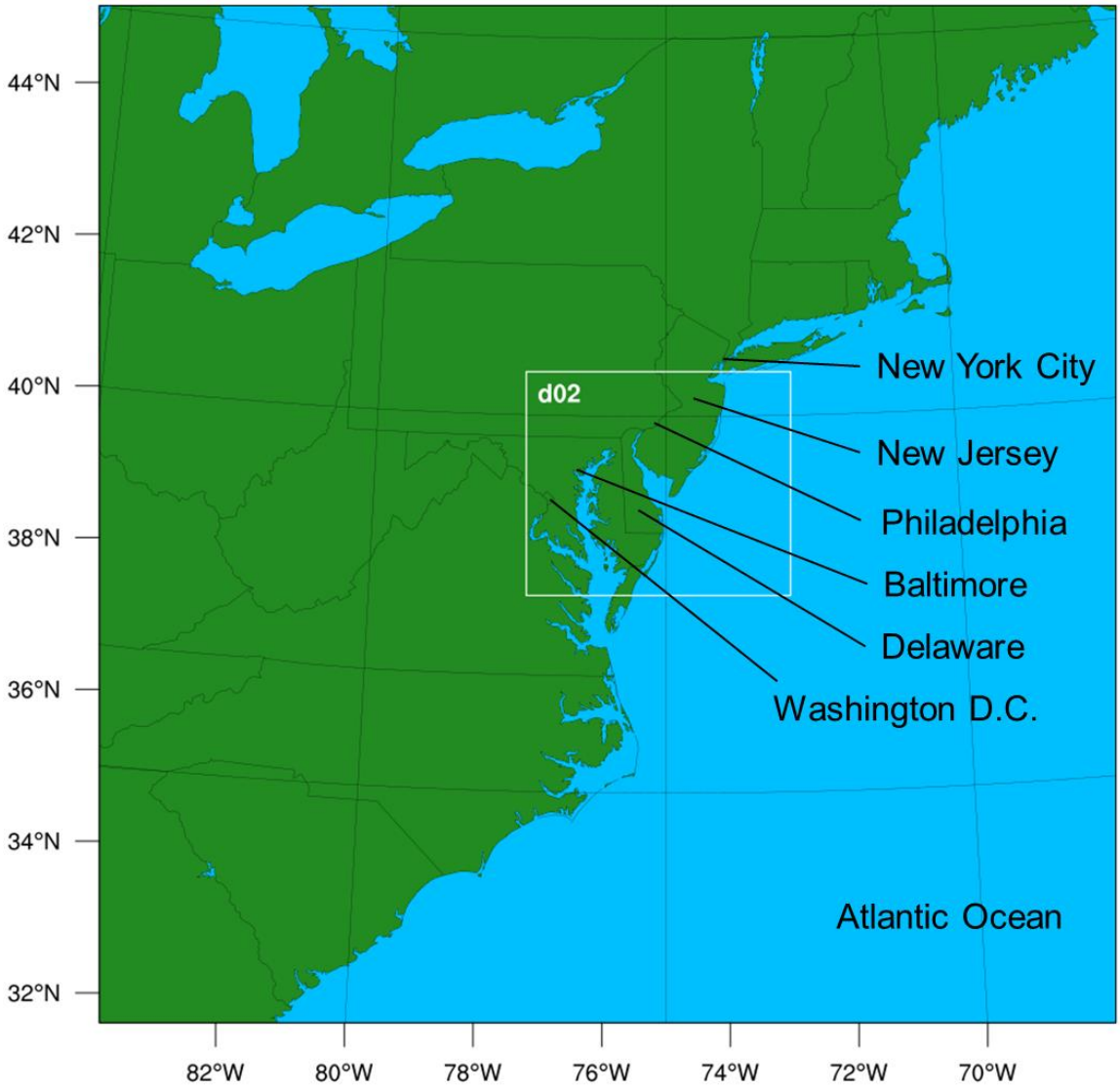

Figure 1: Weather Research and Forecasting Model (WRF) domain configuration

Chapter 2

RESULTS

2.1 Urbanization Increases Summertime Offshore Wind Resources

Urbanization (SSP5_HIST – HIST_HIST) causes increased average summertime (June, July, August) wind speeds over the ocean off New Jersey and Delaware. Surprisingly, much of these impacts are more than 100 km offshore. One potential cause of these changes is decreasing near-surface atmospheric pressure over land which creates a slight increase in the coastal pressure gradient during the summer. Changes in sea level pressure are known to have substantial impacts on average wind speeds (Antonini and Caldeira, 2021): typically, the stronger the pressure gradient, the higher the wind speed. Also, increasing temperatures over land caused by urbanization create a larger temperature gradient between ocean and land during the summer months, which strengthens the sea breeze circulation and can also increase coastal wind speeds.

During the summer, wind speeds 120-m above the ground level (referred to as 120-m wind speeds) increase by 0.4 – 0.6 m/s over most of the ocean grid cells off New Jersey and Delaware in response to increased urbanization (Fig. 2a). These changes correspond

to a 2.5 – 5.0% increase in the amount of time with offshore wind speeds >10.59 m/s. The threshold 10.59 m/s represents the wind speed above which the International Energy Agency (IEA) 15-MW offshore reference turbine (Gaertner et al., 2020), a standard reference turbine used for design studies and collaborative research across different organizations, produces its maximum power output. During the day (8 am – 8 pm local time), 120-m wind speeds directly off the coast increase by 0.6 – 1.0 m/s (Fig. 2b), and overnight (8 pm – 8 am local time) 120-m wind speeds increase by 0.4 – 0.6 m/s further offshore (Fig. 2c). Since wind speeds are the slowest (Hughes and Veron 2015) and energy demand is the highest during summer months in the Mid-Atlantic U.S. (Veron et al., 2018), increases in hub-height (100 – 150 m) winds over the ocean would supply much-needed boosts in energy output to match the high demand. Additionally, increasing temperature enhances the electrical demand for cooling in the summer months. Though changes in wind speed less than 1 m/s might seem small, power density and wind speed are cubically related (Manwell et al., 2009), that is, even small changes in wind speed can have substantial impacts on wind turbine power output. For example, a 0.45 m/s increase in wind speed in the 7-11 m/s range can increase the power output of the reference IEA offshore turbine by more than 12%, or 1.8 MW.

During the winter (December, January, February), spring (March, April, May), and fall (September, October, November), both offshore wind speeds and the mean sea level pressure (MSLP) gradient in the Mid-Atlantic U.S. show minimal changes (<0.2 m/s and 0.1 hectopascals (hPa), respectively) as a result of urbanization. In the summer, the

coastal pressure gradient increases by 0.3 hPa (Fig. 2d), corresponding with increased offshore wind speeds during that time. On summer days, when the sea breeze has the largest impact on local dynamics and near-shore 120-m wind speeds show the largest increases, the coastal pressure gradient strengthens by 0.5 hPa (Fig. 2e). Therefore, larger urbanization impacts on coastal pressure gradients in the summer correspond with larger wind speed impacts, and smaller urbanization impacts on coastal pressure patterns in the winter, spring, and fall correspond with smaller wind speed impacts.

To assess the relationship between urbanization and surface level wind speeds (10-m) and temperatures (2-m) over land, I categorize grid cells in the study area into four classes according to each grid cell's amount of increase in urban land fraction between the beginning and end of the 21st century: 0 – 0.2 (totaling 32.2% of all land grid cells), 0.2 – 0.5 (23.5%), 0.5 – 0.8 (14.1%), 0.8 – 1 (24.2%). Roughly 6% of land area exhibits a decrease in urban land fraction. While the SSP-consistent urban land change data does not contain any decreases in urban land fraction over the 21st century, these minor decreases are caused by the interpolation of different urban datasets onto the WRF grid. I find, overall, annual average 10-m wind speeds decrease and 2-m temperatures increase proportionally to urban land development levels. Impacts on 10-m wind speeds primarily occur in regions with urban land fraction increasing by more than 0.5. Below that threshold, changes are below 0.1 m/s. 2-m temperatures increase by 0.5 – 1.0 ℃ where urban land fraction increases <0.5. In regions with urban land fraction increases between

0.5 – 0.8, 10-m wind speeds decrease by 0.4 m/s, and in areas where urban land fraction increases by >0.8, 10-m wind speeds decrease by 0.7 m/s due to increased surface roughness, and surface temperatures warm by 2.0 ℃ on average . The impacts of urban land expansions on 2-m temperatures do not extend to the ocean, even in high urbanization scenarios like SSP5. This creates a larger temperature gradient between the land and ocean, altering local dynamics during the entire year and especially during the summer when the sea breeze is prevalent.

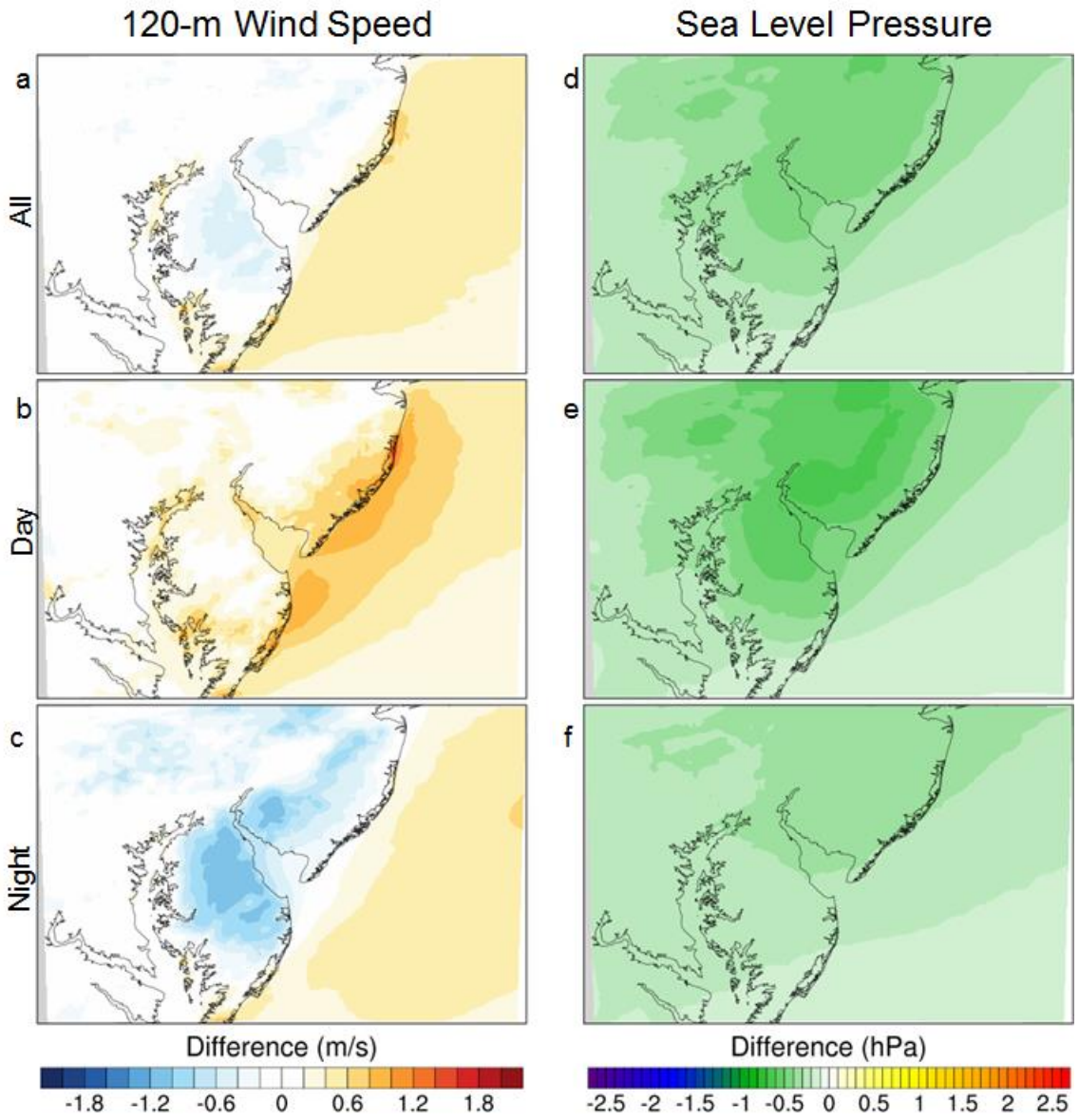

Figure 2: Average summertime (a, b, c) 120-m wind speed and (d, e, f) mean sea level pressure (MSLP) impacts of Shared Socioeconomic Pathway 5 (SSP5) urbanization (SSP5_HIST – HIST_HIST) by the end of the 21st century during all hours, day and night.

2.2 Climate Change Increases Summertime Offshore Wind Resources

Climate change (HIST_RCP8.5 - HIST_HIST) causes larger increases in summertime coastal wind speeds than urbanization due to shifts in the position of the Azores High. Climate change speeds up 120-m summertime wind speeds by 0.8 – 1.4 m/s over the ocean and 0.2 – 0.6 m/s over land (Fig. 3a). The largest increases occur directly to the east and southeast of the New York Bight where numerous offshore wind lease areas are located. These summertime increases are roughly double the increases in other seasons. Climate change and urbanization combined (SSP5_RCP8.5 – HIST_HIST) speed up 120-m summertime wind speeds by 1.8 – 2.2 m/s off the New Jersey coastline and by 1.4 – 1.8 m/s off of Delaware.

Climate change increases the percentage of time when summertime 120-m offshore wind speeds are above 10.59 m/s (reference turbine producing at full power) by 10 – 15 % off the coast of New Jersey and Delaware (Fig. 3c). This increase in offshore wind resources during the summer represents a substantial positive impact on the efficiency of future wind farms. In the winter, this value increases by less than 2.5% over the entire coastal Mid-Atlantic region.

.

The magnitude of offshore wind speed changes is directly related to changes in the coastal mean sea level pressure gradient. In the climate change scenario (HIST_RCP8.5), these changes are linked to a northwesterly shift and strengthening of the Azores High

found in CESM2 output at the end of the 21st century. During the summer, when offshore wind speeds increase the most, coastal pressure gradient changes are the largest (Fig. 3b). The correlation coefficient between monthly changes in 120-m wind speed over the ocean and coastal pressure gradients due to climate change is 0.77 (Fig. 4). This correlation coefficient is 0.90 for the urbanized scenario (SSP5_HIST) and 0.83 for the combined scenario (SSP5_RCP8.5) (Fig. 4).

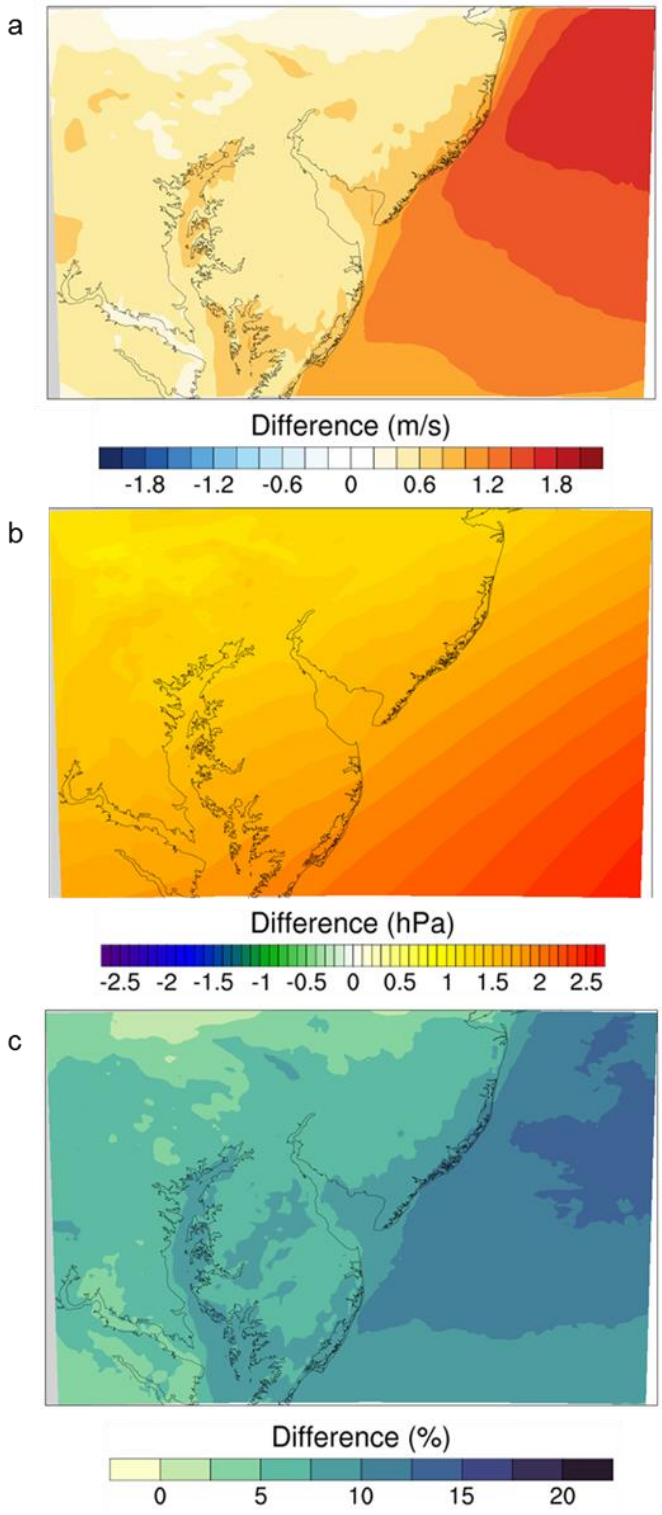
a
Difference (m/s)
-1.8 -1.2 -0.6 0 0.6 1.2 1.8
b
Difference (hPa)
-2.5 -2 -1.5 -1 -0.5 0 0.5 1 1.5 2 2.5
c
Difference (%)
0 5 10 15 20

Figure 3: Climate change impacts (HIST_RCP8.5 - HIST_HIST) on: (a) summertime 120-m wind speeds, (b) mean sea level pressure (MSLP), and (c) the percentage of time with 120-m wind speeds >10.59 m/s.

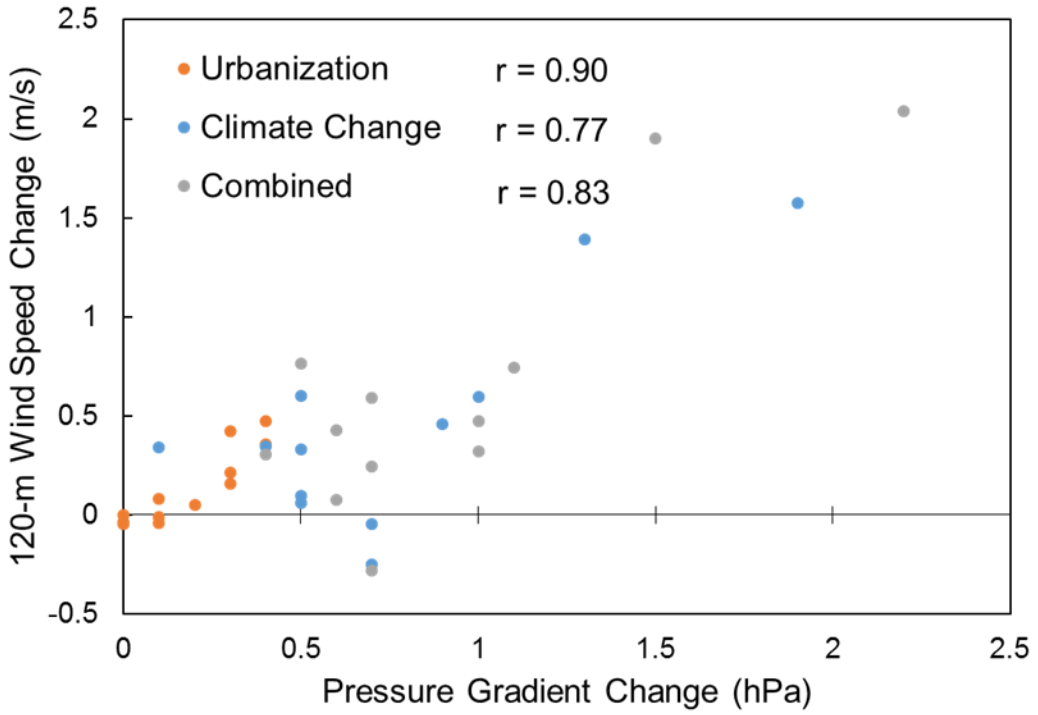

Figure 4: Correlation between monthly changes in 120-m wind speeds and the coastal pressure gradient due to urbanization (SSP5_HIST – HIST_HIST), climate change (HIST_RCP8.5 – HIST_HIST), and both combined (SSP5_RCP8.5 – HIST_HIST)

2.3 Conflicting Impacts of Urbanization and Climate Change on Sea Breeze Circulation

For sea breeze circulation, I analyze the east-west wind speed as a proxy, because the coastlines of the Mid-Atlantic U.S. are oriented in a nearly north-south direction. Overall, urbanization increases the strength of the sea breeze while climate change weakens it. In the following paragraphs describing impacts on the sea breeze, I focus on the summer

daytime (8am – 8pm local time) because the sea breeze is the most prevalent (Hughes and Veron, 2015) and I find larger impacts due to urbanization and climate change during that time.

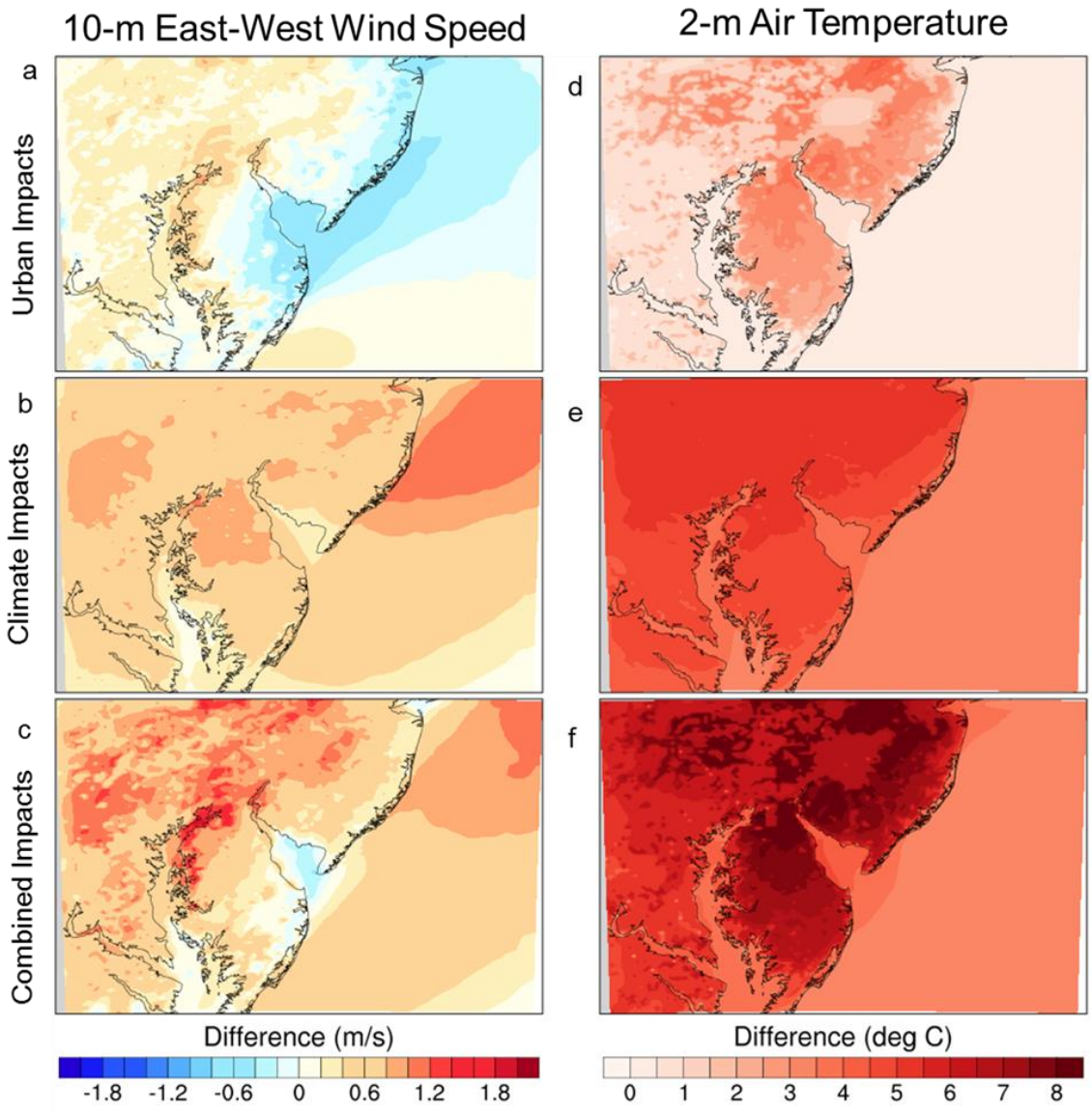

Figure 5: Urbanization (SSP5_HIST – HIST_HIST), climate change (HIST_RCP8.5 – HIST_HIST), and combined (SSP5_RCP8.5 – HIST_HIST) impacts on (a, b, c) daytime summer east-west 10-m wind speed and (d, e, f) 2-m temperature.

Urbanization (SSP5_HIST – HIST_HIST) strengthens the sea breeze through changes in local temperature gradients in the coastal Mid-Atlantic U.S. on summer days. The largest increases in easterly winds, which represent a more robust sea breeze circulation, occur in the Delaware Bay between New Jersey and Delaware (0.6 m/s) and along the coastlines of southern New Jersey and Delaware (0.4 m/s) (Fig. 5a). Increasing easterly winds can be found as far as 100-km offshore, demonstrating the permeating urbanization effects during summer days. The 2-m air temperatures over land increase by 1.0 ℃ on average and by up to 3.5 ℃ in southern New Jersey and Delaware due to the urban heat island effect (Fig. 5d). Temperatures over the ocean are not affected by urbanization, creating a larger temperature gradient between the ocean and land initiating a stronger pressure gradient oriented perpendicular to the coastline.

Climate change (HIST_RCP8.5 – HIST_HIST) increases the westerly 10-m wind speeds, directly counteracting and suppressing the development and propagation of the sea breeze (Fig. 5b). The largest impacts (>1.0 m/s) are found off of the New Jersey coastline. The increased westerly component of coastal winds is associated with the northerly shift of

the Azores High during the summer, which increases the pressure gradient in the southeast-northwest direction and strengthens the prevailing southwesterly winds. In the combined scenario (SSP5_RCP8.5), the enhanced westerly flow due to climate change exceeds increases in easterly flow due to urbanization, resulting in a mild weakening of the sea breeze along most of the Mid-Atlantic U.S. coast. (Fig. 5c). Further research is needed to fully understand factors and dynamics influencing the strengths of the contradictory forces from urbanization and climate change relating to the sea breeze circulation.

2.4 Climate Change and Urbanization Both Increase Extreme Heat Events

Both climate change and urbanization notably increase air temperatures in the Mid-Atlantic U.S. Climate change causes average summer 2-m temperature increases between 4.5 – 5.0 ℃ in coastal regions and 5.0 – 5.5 ℃ farther inland. Urbanization causes 2 – 3.5 ℃ over urbanizing areas during the same time period. The combined impacts of climate change and urbanization (SSP5_RCP8.5 – HIST_HIST) cause surface temperatures to increase by as much as 7 – 8.5 ℃ over urbanizing areas.

The percentage of time with surface temperatures above 35 ℃ (95 ℉) is an indicator of extreme heat for public health concerns. In the Mid-Atlantic U.S., the combined effects

of climate change and urbanization causes the percentage of hours in the summer >35 ℃ to increase 10 – 40% (Fig. 6a). The increased time in extreme heat conditions is particularly concerning when the weakening of sea breeze associated with climate change, which creates a decrease in cooling, is considered. For comparison, in the historical scenario (HIST_HIST), the percentage of time with summertime 2-m air temperatures >35 ℃ is <5% throughout most of the domain and between 5 – 10% near Philadelphia, Baltimore, and Washington D.C. While the interaction between climate change and urbanization in the combined scenario is minimal for other variables, this interaction causes the fraction of time spent in extreme heat conditions to be 5 – 20% higher over urbanizing areas (Fig. 6b).

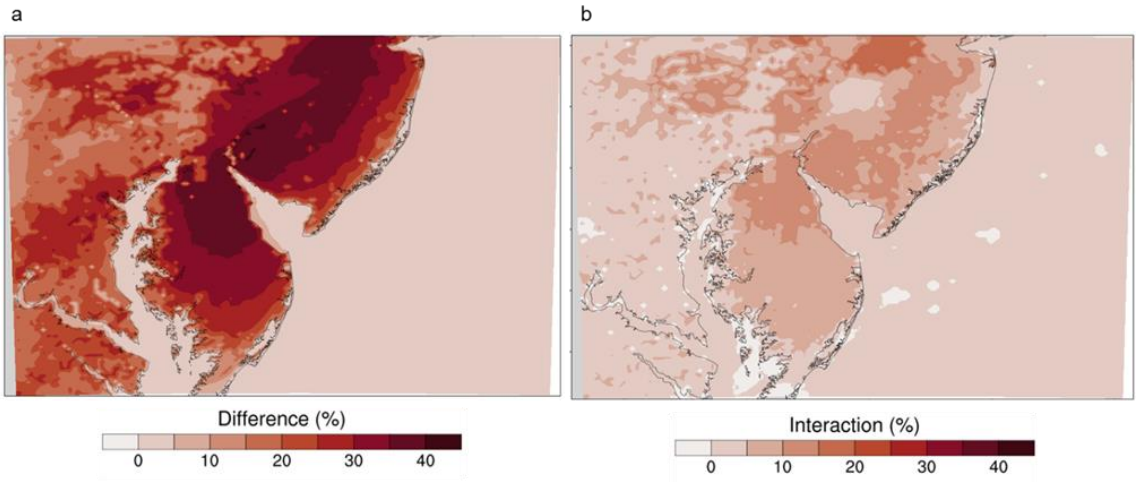

Figure 6: (a) Summertime impacts of urbanization and climate change (SSP5_RCP8.5 – HIST_HIST) on the fraction of time with 2-m air temperatures >35℃ and (b) the interaction ((SSP5_RCP8.5 – HIST_RCP8.5) – (SSP5_HIST – HIST_HIST) between urbanization and climate change in the combined scenario.

Chapter 3

DISCUSSION

Increasing summertime coastal winds associated with urbanization and climate change are encouraging for the developing offshore wind industry. Even in future scenarios with less urban development and smaller climate impacts, it is likely that coastal wind speeds will increase to some degree due to synoptic-scale temperature and pressure patterns from climate change, and increasing pressure gradients perpendicular to the Mid-Atlantic U.S. coastline due to urbanization. At the same time, much higher summer temperatures will lead to increased air-conditioning usage and a potentially much higher energy demand. Balancing the magnitudes of the two conflicting effects in the study area, increases in available offshore wind resources would likely be substantially smaller than increases in energy demands, a problem that may be exacerbated by potential population growth. In the SSP5-consistent urbanization scenario, urban land fraction in rural southern New Jersey and Delaware increases by >0.8. The large increases in urban heat island effects and subsequently air-conditioning-related energy demands would be very difficult to meet through renewable energy alone. As the offshore wind industry develops in the U.S. and begins to account for a larger portion of regional electricity generation, it will be crucial to monitor changing urban and climate conditions and continue to evaluate future projections.

These findings differ from previous studies considering climate change or urbanization impacts on coastal wind resources and sea breeze circulation (no research has considered both together). For coastal winds, several studies predict decreases in annual average wind speeds in the coastal Mid-Atlantic U.S. (Martinez and Iglesias, 2022, Costoya et al., 2020, Pryor et al., 2020, Johnson and Erhardt, 2016), while I find increases primarily due to amplified summer average wind speeds. The difference in findings may be a result of anticipated future shifts of large-scale pressure patterns (i.e., Azores High), which may evolve differently in other modeling studies. The contrary findings may have also arisen because the fine-resolution simulations capture changes in local dynamics that previous coarser-resolution continental-scale simulations could not resolve. For sea breeze, one idealized study examining the city of Houston finds urbanization to slow sea breeze propagation and surface wind speed due to increased surface roughness (Chen et al., 2011). In contrast, I find mixed effects of urbanization on surface wind speeds, which decreases over Delaware and increases over New Jersey. At 120 meters above the ground, urbanization increases wind speeds throughout the coastal Mid-Atlantic U.S., especially on summer days (Fig. 2b). This is a young evolving interdisciplinary literature body. More high-resolution simulations are needed for understanding influences of various factors at play, such as, geographical locations, model resolutions, and input data.

Due to a northwesterly shift of the Azores High in the summer (southeasterly in winter), surface pressure increases (decreases) by as much as 2.0 (2.5) hPa in the coastal Mid-Atlantic U.S. These changes are in contrast to existing observational studies. For

example, one study (Taylor et al., 2012) finds a northerly shift in the Azores High over the entire year, while others (Falarz, 2019, Iqbal et al., 2019) find a pronounced northerly shift in January. These observational changes are linked to a strengthening Hadley circulation due to global warming (Iqbal et al., 2019). One study finds a general southwesterly shift of the Azores High in the summer, while an individual 10-year period may exhibit a different tendency (e.g., an easterly shift) (Falarz, 2019). Altogether, these observational studies suggest it is possible that the direction of the Azores High shifts during the 10-year future period of study (2090-2099) might somewhat differ from longer-term trends. However, both this and other studies (Iqbal et al., 2019, Taylor et al., 2012) concur that the location and the strength of the Azores High can have considerable regional impacts on temperature, pressure, wind speed and direction. Therefore, the high uncertainty of future pressure pattern trends demands important future consideration.

This exercise of co-investigating regional impacts of urbanization and climate change provides new insights to the broader field of regional climate modeling. Firstly, the impacts of large-scale urbanization on wind speeds are not only found in regions directly surrounding urban areas, but as far as 100 km offshore (Fig. 2 and 5) . Further simulations are needed to determine whether the wide-reaching urbanization impacts found here are limited to coastal regions, where wind speed is particularly sensitive to changes in temperature gradients, or if they are found further inland as well. Secondly, the increasing coastal wind speed from climate change found here may be specific to the shifting pressure patterns in this region and may not be generalizable to other regions.

Nonetheless, I find large variability between offshore and onshore climate impacts on wind speed (Fig. 3a) that are not found in previous studies (Martinez and Iglesias, 2022, Pryor et al., 2020), demonstrating the added value of increasing spatial resolution for detailed wind projections.

Chapter 4

METHODS

4.1 Climate Forcing Data

In this study, Community Earth System Model Version 2 (CESM2) (Danabasoglu et al., 2020) output is dynamically downscaled using the Weather Research and Forecasting (WRF) model version 4.2 (Skamarock et al., 2019) as a regional climate model (RCM). CESM2 is developed by the National Center for Atmospheric Research (NCAR) and is one of the earth system models used in the Coupled Model Intercomparison Project Phase 6 (CMIP6) (Eyring et al., 2016) showing minimal surface wind speed bias in the equatorial Atlantic (Richter and Tokinaga, 2020). Dynamically downscaling CESM2 using WRF has been shown to produce realistic climate simulations and this GCM-RCM pair has recently been integrated into an accessible regional earth system modeling framework (Fu et al., 2021) along with the Regional Ocean Modeling System (ROMS) (Haidvogel et al., 2008).

The output from the 40-km top, limited chemistry version of CESM2 (CESM2-CAM6) with a horizontal resolution of 1.26° (longitude) x 0.94° (latitude) is used as forcing data in this study. Historical climate forcing from the early 21st century (2005-2014) is obtained from the r11i1p1f1 variant of the CESM2-CAM6 historical run (1850-2014). Global

climate conditions at the end of the 21st century (2090-2099) use the r11i1p1f1 ScenarioMIP variant of CESM2-CAM6. The RCP8.5 scenario is selected here to simulate the regional impacts of uninhibited climate change and urbanization in the coastal Mid-Atlantic U.S. The drastic land use changes predicted under the SSP5 scenario in this region (Fig. 1) create a unique opportunity to investigate the effects of coastal urbanization within the megalopolis of the Northeastern U.S.

In order to downscale CESM2 using WRF, I follow the methods from a recent paper (Rahimi et al., 2022). Intermediate files are needed to be read into the WRF Pre-Processing System (WPS). These binary intermediate files must contain the 16 atmospheric, oceanic, and land-based variables that WPS requires to run. Conversion of CESM2 output to the required intermediate format took considerable processing, including horizontal interpolation to the Community Atmosphere Model (CAM) grid and vertical interpolation of atmospheric variables to 25 pressure levels ranging from 1000 – 10 hpa. Finally, soil moisture and soil temperature variables from CESM2 are converted to the soil levels required by WPS and intermediate binary files are created for every 6-hour period throughout each of the 10-year model simulations.

4.2 Urban Land Change Data

I represent spatial urban land change in the WRF domains using a new dataset of SSP-consistent global decadal 1-km urban land fraction projections throughout the 21st century (Gao and Pesarasi, 2021). The dataset is produced by the first and the most current empirically-grounded long-term spatial urban land modeling framework, CLUBS-SELECT (CLUBS: Country-Level Urban Buildup Scenario, Gao and O'Neill, 2020; SELECT: Spatially-Explicit, Long-term, Empirical City developmenT, Gao and O'Neill, 2019), taking advantage of the 15 best available global datasets on urbanization and its driving forces. The spatial urban land fraction projections are integrated into the static land use files for the urbanized WRF scenarios (SSP5_HIST, SSP5_RCP8.5), and I represent the end-of-century urbanization as the SSP5 urban land conditions in the year 2100 (Fig. 7c,d). For scenarios using historical urban conditions, the default land use fraction in WRF is used, which is NASA's Moderate Resolution Imaging Spectroradiometer (MODIS) satellite-derived land use data (Justice et al., 2002, Fig. 7a,b).

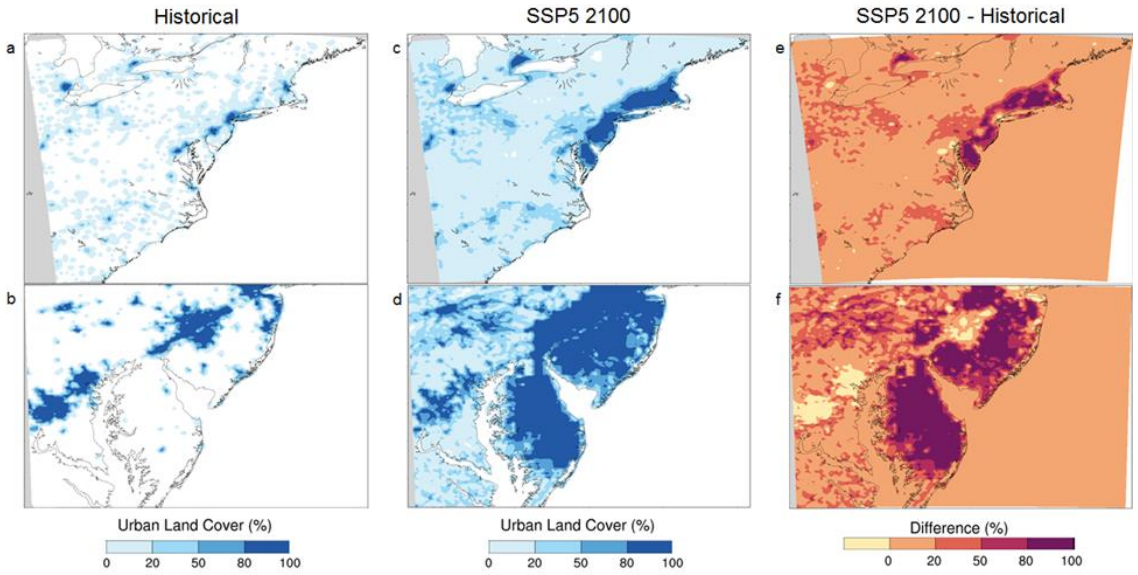

Figure 7: (a and b) Historical urban land cover (%) in model domains from NASA's Moderate Resolution Imaging Spectroradiometer (MODIS data), (c and d) Shared Socioeconomic Pathway 5 (SSP5) 2100 urban land cover (%), and (e and f) SSP5 2100 urban land cover minus historical land cover (%).

While the effects of future urbanization based on SSP scenarios are included in the EOC CESM2 data used in this study (Danabasoglu et al., 2020, Oleson and Feddema, 2020, Jiang and O'Neill, 2017, O'Neill et al., 2016), these changes are not represented in the WRF domains. To integrate urbanization into WRF, I apply the same method as Bukovsky et al., 2021. SSP5 urban land fraction data are first interpolated onto new grids, altering their initial spatial resolution to fit WRF grid spacing. Next, urban fraction differences between SSP5 2100 and MODIS data are calculated and integrated into the urbanized scenarios (SSP5_HIST and SSP5_RCP8.5). These differences are also used to update the dominant land use category for each grid cell. Finally, each of the other land use fractions are scaled down proportionally to adjust for the changes in urban land.

4.3 WRF Configuration and Simulated Scenarios

I simulate four regional climate scenarios in this study aimed at investigating the independent and combined impacts of urbanization and climate change on coastal wind patterns in the Mid-Atlantic U.S. The scenarios are as follows:

- HIST_HIST, historical urban land extent (MODIS) and climate conditions (2005 – 2014)
- SSP5_HIST, SSP5 urban land extent in 2100 and historical climate conditions
- HIST_RCP8.5, historical urban land extent and EOC RCP8.5 climate conditions (2090 – 2099), and
- SSP5_RCP8.5, urban land extent in 2100 and EOC RCP8.5 climate conditions

For each scenario, the same RCM configuration and suite of physics options (Table 1) are used. In order to downscale the coarse CESM2 forcing data to a high resolution simulation, I use two, two-way nested domains in WRF. The outer domain (15-km resolution, 101 east-west x 101 north-south grid points) is centered on the eastern U.S. and the inner domain (3-km resolution, 131 east-west x 111 north-south grid points) spans the coastal Mid-Atlantic U.S. (Fig. 1). At a spatial resolution of 3 km, WRF is able to resolve mesoscale processes which play an important role in local wind patterns. An integration time step of 90 seconds is used (consistent with 6 x dx rule of thumb), and adaptive time-stepping is applied in order to save on computational costs (Hutchinson, 2007). In order to realistically capture the entire troposphere in these regional climate simulations, I use 54 vertical levels and a model top at 50 hPa. Simulations were

performed on NCAR's supercomputer Cheyenne (Computational and Information Systems Laboratory, 2019) and CESM2 data were acquired using the NCAR CMIP Analysis Platform (more details in acknowledgements).

Table 1: Weather Research and Forecasting (WRF) model physics options

Planetary Boundary Layer Physics	MYNN2.5
Shortwave Radiation	RRTMG
Longwave Radiation	RRTMG
Land Surface Physics	Noah-MP Land Surface Model
Surface Layer Physics	Eta Similarity Scheme
Microphysics	Morrison 2-moment Scheme
Cumulus Parametrization	Kain-Fritsch Scheme (Parent Domain)

Since runoff and soil-moisture are not a focus of this study, the model spin-up time leading up to the simulations is two months. Each of the simulations run continuously for the entire 10 years and two months without any cold starts. In order to navigate wall-time limitations for job submissions, restart runs were initiated every 12 hours of run-time. Spectral nudging, which can be used to prevent RCM drift from boundary conditions, is not used in this study for several reasons. The outer domain used here (1515 km) is near the bottom limit for the typical size of studies using spectral nudging and it is more-

commonly used in historical simulations (Schaaf et al., 2017). It has been found to produce minimal changes in small domains (Schaaf et al., 2017) and is avoided in one high-resolution regional climate simulation of the Northeastern U.S. to prevent artificial signals introduced at regional scales (Komurcu et al., 2018). I do not use an urban model due to the high-sensitivity to parameters that are unique to each city (Chen et al., 2010, Salamanca et al., 2011) although the Building Effect Parametrization (BEP) has been shown to improve the simulation of some urban environments and may be useful to consider in future work (Barlage et al., 2016). The physics options used in this study are targeted to optimize the accuracy of WRF in the coastal Mid-Atlantic U.S. based on a recent sea breeze study in Delaware (Allen, 2021) (Table 1).

4.4 Analyzing the Effects of Urbanization and Climate Change

Various analysis methods are applied to the RCM output to evaluate the impacts of urbanization and climate change on coastal wind patterns in the Mid-Atlantic U.S. Output is available every hour from the inner domain and every 6 hours from the outer domain, totaling 12 TB of data spanning the 40 years of simulations. The list of variables assessed includes: 120-m wind speed, 10-m wind speed, 2-m air temperature, 2-m dew point temperature, MSLP, planetary boundary layer height (PBLH), and east-west 10-m winds. The 120-m wind speed is vertically interpolated from the lowest few layers of wind speed output using a built-in NCL interpolation function and the 10-m wind speed is calculated using the east-west and north-south components of the wind at 10 meters.

To quantify the independent and combined effects from urbanization and climate change, I compute annual and seasonal averages in each grid cell, and subtract the historical scenario (HIST_HIST) from the perturbation scenarios (SSP5_HIST, HIST_RCP8.5 and SSP5_RCP8.5) for each variable. These seasonal and annual differences reveal the spatial impacts of each scenario compared to the historical scenario. In order to better characterize these spatial differences, I performed averages of 120-m wind speed and 2-m temperature across the entire domain for land and ocean grid cells. For the same reason, percentage difference calculations between scenarios is avoided to prevent falsely amplified results over the land, where wind speeds are typically lower.

The amount of time 120-m wind speed and 2-m temperature are above a certain threshold is assessed to determine changes in wind resources and extreme heat events. A wind speed threshold of 10.59 m/s is used to determine how frequently offshore winds are at or above the rated wind speed for the International Energy Agency (IEA) offshore reference turbine (Gaertner et al., 2020). This 15-Megawatt turbine designed by collaborators at the National Renewable Energy Laboratory (NREL), Technical University of Denmark (DTU), and the University of Maine is selected to represent the near future of rapidly growing offshore wind turbine designs. As a metric for extreme heat events, the percentage of time when surface temperature >35 ℃ (95 ℉) is calculated during summer months. This calculation includes nighttime hours and provide more information on the

duration of extreme heat conditions than a simple count of days with daily maximum temperatures above a certain threshold.

Offshore wind speed distributions, analysis based on urban land fraction, and interaction between scenarios are considered in addition to the spatial and threshold analyses. Distributions of annual and summer wind distributions at 120-m over the ocean are analyzed to determine the impacts of climate change and urbanization on offshore wind resources. The frequency of wind speeds at 1-m/s intervals between 0-25 m/s are calculated and compared for each scenario. In order to identify the specific impacts of changing urbanization on surface winds and temperature, the land grid cells are categorized by the following urban land fraction changes: 0.0 – 0.2, 0.2 – 0.5, 0.5 – 0.8, 0.8 – 1.0. Surface temperature and wind speed from each scenario are then averaged by class and compared to each other. Finally, the level of interaction between urbanization and climate change is determined by performing the following calculation on the grid-cell average of each variable: (SSP5_RCP8.5 – HIST_RCP8.5) – (SSP5_HIST – HIST_HIST). This calculation produces a non-zero result if there is an interaction between the urbanization and climate change. It should be noted that the level of interaction can also be determined using the following equation: (SSP5_RCP8.5 – SSP5_HIST) – (HIST_RCP8.5 – HIST_HIST).

REFERENCES

Antonini, E. G. A., & Caldeira, K. (2021). Atmospheric pressure gradients and Coriolis forces provide geophysical limits to power density of large wind farms. *Applied Energy*, *281*. https://doi.org/10.1016/j.apenergy.2020.116048

Barlage, M., Miao, S., & Chen, F. (2016). Impact of physics parameterizations on high-resolution weather prediction over two chinese megacities. Journal of Geophysical Research: Atmospheres, 121(9), 4487–4498. https://doi.org/10.1002/2015JD024450

Bowers, L. A. (2004). The effect of sea surface temperature on sea breeze dynamics along the coast of New Jersey (Doctoral dissertation, Rutgers University).

Bukovsky, M. S., Gao, J., Mearns, L. O., & O'Neill, B. C. (2021). SSP-based land-use change scenarios: A critical uncertainty in future regional climate change projections. *Earth's Future*, 9, e2020EF001782. https://doi.org/10.1029/2020EF001782

Carvalho, D., Rocha, A., Gómez-Gesteira M, & Silva Santos, C. (2017). Potential impacts of climate change on european wind energy resource under the cmip5 future climate projections. *Renewable Energy*, *101*, 29–40. https://doi.org/10.1016/j.renene.2016.08.036

Chen, F., Kusaka, H., Bornstein, R., Ching, J., Grimmond, C.S.B., Grossman-Clarke, S., Loridan, T., Manning, K.W., Martilli, A., Miao, S., Sailor, D., Salamanca, F.P., Taha, H., Tewari, M., Wang, X., Wyszogrodzki, A.A. and Zhang, C. (2011), The integrated WRF/urban modelling system: development, evaluation, and applications to urban environmental problems. Int. J. Climatol., 31: 273-288. https://doi.org/10.1002/joc.2158

Chen, F., Miao, S., Tewari, M., Bao, J.-W., & Kusaka, H. (2011). A numerical study of interactions between surface forcing and sea breeze circulations and their effects on stagnation in the greater houston area. Journal of Geophysical Research, 116(D12). https://doi.org/10.1029/2010JD015533

Chen, L. (2020). Impacts of climate change on wind resources over north america based on na-cordex. *Renewable Energy*, *153*, 1428–1438.

Chen, X., Jeong, S., Park, H., Kim, J., & Park, C. R. (2020). Urbanization has stronger impacts than regional climate change on wind stilling: A lesson from South Korea. *Environmental Research Letters*, *15*(5). https://doi.org/10.1088/1748-9326/ab7e51

Childs, P. P., & Raman, S. (2005). Observations and numerical simulations of urban heat island and sea breeze circulations over new york city. *Pure and Applied Geophysics : Pageoph*, *162*(10), 1955–1980. https://doi.org/10.1007/s00024-005-2700-0

Computational and Information Systems Laboratory. 2019. Cheyenne: HPE/SGI ICE XA System (University Community Computing). Boulder, CO: National Center for Atmospheric Research. doi:10.5065/D6RX99HX.

Costoya, X., deCastro, M., Carvalho, D., & Gómez-Gesteira, M. (2020). On the suitability of offshore wind energy resource in the united states of america for the 21st century. *Applied Energy*, *262*. https://doi.org/10.1016/j.apenergy.2020.114537

Craig, M. T., Losada Carreño Ignacio, Rossol, M., Hodge, B.-M., Brancucci, C., & National Renewable Energy Lab. (NREL), Golden, CO (United States). (2019). Effects on power system operations of potential changes in wind and solar generation potential under climate change. Environmental Research Letters, 14(3). https://doi.org/10.1088/1748-9326/aaf93b

Danabasoglu, G., Lamarque, J.-F., Bacmeister, J., Bailey, D. A., DuVivier, A. K., Edwards, J., et al. (2020). The Community Earth System Model Version 2 (CESM2). *Journal of Advances in Modeling Earth Systems*, 12, e2019MS001916. https://doi.org/10.1029/2019MS001916

Daniel, M., Lemonsu, A., Déqué, M. *et al.* Benefits of explicit urban parameterization in regional climate modeling to study climate and city interactions. *Clim Dyn* **52,** 2745–2764 (2019). https://doi.org/10.1007/s00382-018-4289-x

Davy, R., Gnatiuk, N., Pettersson, L., & Bobylev, L. (2018). Climate change impacts on wind energy potential in the european domain with a focus on the black sea. *Renewable and Sustainable Energy Reviews: Part 2*, *81*, 1652–1659. https://doi.org/10.1016/j.rser.2017.05.253

Eyring, V., Bony, S., Meehl, G. A., Senior, C. A., Stevens, B., Stouffer, R. J., Taylor, K. E., & Lawrence Livermore National Lab. (LLNL), Livermore, CA (United States). (2016). Overview of the coupled model intercomparison project phase 6 (cmip6) experimental design and organization. Geoscientific Model Development (Online), 9(5). https://doi.org/10.5194/gmd-9-1937-2016

Friedl, M. A., McIver, D. K., Hodges, J. C. F., Zhang, X. Y., Muchoney, D., Strahler, A. H., Woodcock, C. E., Gopal, S., Schneider, A., Cooper, A., Baccini, A., Gao, F., & Schaaf, C. (2002). Global land cover mapping from MODIS: algorithms and early results.

Remote Sensing of Environment, *83*(1–2), 287–302. https://doi.org/10.1016/S0034-4257(02)00078-0

Fu, D., Small, J., Kurian, J., Liu, Y., Kauffman, B., Gopal, A., Ramachandran, S., Shang, Z., Chang, P., Danabasoglu, G., Thayer-Calder, K., Vertenstein, M., Ma, X., Yao, H., Li, M., Xu, Z., Lin, X., Zhang, S., & Wu, L. (2021). Introducing the new regional community earth system model, r-cesm. *Bulletin of the American Meteorological Society*, *1-53*, 1–53. https://doi.org/10.1175/BAMS-D-20-0024.1

Gaertner, Evan, Jennifer Rinker, Latha Sethuraman, Frederik Zahle, Benjamin Anderson, Garrett Barter, Nikhar Abbas, Fanzhong Meng, Pietro Bortolotti, Witold Skrzypinski, George Scott, Roland Feil, Henrik Bredmose, Katherine Dykes, Matt Shields, Christopher Allen, and Anthony Viselli. 2020. Definition of the IEA 15-Megawatt Offshore Reference Wind. Golden, CO: National Renewable Energy Laboratory. NREL/TP-5000-75698. https://www.nrel.gov/docs/fy20osti/75698.pdf

Gao, J., O'Neill, B.C. Mapping global urban land for the 21st century with data-driven simulations and Shared Socioeconomic Pathways. *Nat Commun* **11,** 2302 (2020). https://doi.org/10.1038/s41467-020-15788-7

Gao, J., Pesaresi, M. Downscaling SSP-consistent global spatial urban land projections from 1/8-degree to 1-km resolution 2000–2100. *Sci Data* **8,** 281 (2021). https://doi.org/10.1038/s41597-021-01052-0

Haidvogel, D. B., Arango, H., Budgell, W. P., Cornuelle, B. D., Curchitser, E., Di Lorenzo, E., Fennel, K., Geyer, W. R., Hermann, A. J., Lanerolle, L., Levin, J., McWilliams, J. C., Miller, A. J., Moore, A. M., Powell, T. M., Shchepetkin, A. F., Sherwood, C. R., Signell, R. P., Warner, J. C., & Wilkin, J. (2008). Ocean forecasting in terrain-following coordinates: formulation and skill assessment of the regional ocean modeling system. Journal of Computational Physics, 227(7), 3595–3624. https://doi.org/10.1016/j.jcp.2007.06.016

Haupt, S. E., Copeland, J., Cheng, W. Y. Y., Zhang, Y., Ammann, C., & Sullivan, P. (2016). A method to assess the wind and solar resource and to quantify interannual variability over the united states under current and projected future climate. *Journal of Applied Meteorology and Climatology*, *55*(2), 345–363.

Hou, A., Ni, G., Yang, H., & Lei, Z. (2013). Numerical analysis on the contribution of urbanization to wind stilling: An example over the greater Beijing metropolitan area. *Journal of Applied Meteorology and Climatology*, *52*(5), 1105–1115. https://doi.org/10.1175/JAMC-D-12-013.1

Hutchinson, T. A. (2007, May). An adaptive time-step for increased model efficiency. In *Extended Abstracts, Eighth WRF Users' Workshop* (p. 4).

Iacono, M. J., Delamere, J. S., Mlawer, E. J., Shephard, M. W., Clough, S. A., & Collins, W. D. (2008). Radiative forcing by long-lived greenhouse gases: Calculations with the AER radiative transfer models. *Journal of Geophysical Research: Atmospheres*, *113*(D13), 13103. https://doi.org/10.1029/2008JD009944

Janjic, Z. I., 1994: The step-mountain Eta coordinate model: further developments of the convection, viscous sublayer and turbulence closure schemes. *Mon. Wea. Rev.*, **122**, 927–945. doi:10.1175/1520-0493(1994)122<0927:TSMECM>2.0.CO;2

Jiang, L., & O'Neill, B. C. (2017). Global urbanization projections for the Shared Socioeconomic Pathways. *Global Environmental Change*, *42*, 193–199. https://doi.org/10.1016/J.GLOENVCHA.2015.03.008

Johnson, D. L., & Erhardt, R. J. (2016). Projected impacts of climate change on wind energy density in the united states. *Renewable Energy*, *85*, 66–73. https://doi.org/10.1016/j.renene.2015.06.005

Justice, C. O., Townshend, J. R. G., Vermote, E. F., Masuoka, E., Wolfe, R. E., Saleous, N., Roy, D. P., & Morisette, J. T. (2002). *An overview of MODIS Land data processing and product status*. http://www.edc.usgs.gov/programs/sddm/modisdist/index.shtml

Kain, J. S. (2004). The kain-fritsch convective parameterization: an update. Journal of Applied Meteorology (1988-2005), 43(1), 170–181.

Kalnay, E., & Cai, M. (2003). Impact of urbanization and land-use. Nature, 425(6953), 102–102.

Karnauskas, K. B., Lundquist, J. K., & Zhang, L. (2018). Southward shift of the global wind energy resource under high carbon dioxide emissions. *Nature Geoscience*, *11*(1), 38–43. https://doi.org/10.1038/s41561-017-0029-9

Komurcu, M., Emanuel, K. A., Huber, M., & Acosta, R. P. (2018). High-resolution climate projections for the northeastern United States using dynamical downscaling at convection-permitting scales. Earth and Space Science, 5, 801–826. https://doi.org/10.1029/2018EA000426

Kriegler, E., Bauer, N., Popp, A., Humpenöder, F., Leimbach, M., Strefler, J., Baumstark, L., Bodirsky, B. L., Hilaire, J., Klein, D., Mouratiadou, I., Weindl, I., Bertram, C., Dietrich, J.-P., Luderer, G., Pehl, M., Pietzcker, R., Piontek, F., Lotze-Campen, H., … Energy, and R. (2017). Fossil-fueled development (ssp5): an energy and resource intensive scenario for the 21st century. *Global Environmental Change*, *42*.

Manwell, J. F., McGowan, J. G., & Rogers, A. L. (2009). *Wind energy explained : theory, design and application* (2nd ed.). Wiley.

Martinez, A., & Iglesias, G. (2022). Climate change impacts on wind energy resources in north america based on the cmip6 projections. *Science of the Total Environment: Part 2*, *806*. https://doi.org/10.1016/j.scitotenv.2021.150580

McCabe, E. J. (2021). *Objective Methodology to Identify the Sea Breeze Circulation and Associated Low-Level Jet in the New York Bight* (Doctoral dissertation, State University of New York at Albany).

Morrison, H., Thompson, G., & Tatarskii, V. (2009). Impact of Cloud Microphysics on the Development of Trailing Stratiform Precipitation in a Simulated Squall Line: Comparison of One- and Two-Moment Schemes. *Monthly Weather Review*, *137*(3), 991–1007. https://doi.org/10.1175/2008MWR2556.1

Nakanishi, M., & Niino, H. (2009). Development of an Improved Turbulence Closure Model for the Atmospheric Boundary Layer. *Journal of the Meteorological Society of Japan. Ser. II*, *87*(5), 895–912. https://doi.org/10.2151/JMSJ.87.895

Niu, G. Y., Yang, Z. L., Mitchell, K. E., Chen, F., Ek, M. B., Barlage, M., Kumar, A., Manning, K., Niyogi, D., Rosero, E., Tewari, M., & Xia, Y. (2011). The community Noah land surface model with multiparameterization options (Noah-MP): 1. Model description and evaluation with local-scale measurements. *Journal of Geophysical Research: Atmospheres*, *116*(D12), 12109. https://doi.org/10.1029/2010JD015139

Offshore wind - it's all at sea: the iea's latest world energy outlook special report reveals a burgeoning technology that today has a total capacity of 23 gw, though accounting for only 0.3% of global electricity generation, but has the potential to become a mainstay of the world's power supply.(wind power / offshore wind outlook). (2019). *Modern Power Systems*, *39*(11), 10.

Oleson, K. W., & Feddema, J. (2020). Parameterization and Surface Data Improvements and New Capabilities for the Community Land Model Urban (CLMU). *Journal of Advances in Modeling Earth Systems*, *12*(2). https://doi.org/10.1029/2018MS001586

O'Neill, B. C., Tebaldi, C., van Vuuren, D. P., Eyring, V., Friedlingstein, P., Hurtt, G., Knutti, R., Kriegler, E., Lamarque, J.-F., Lowe, J., Meehl, G. A., Moss, R., Riahi, K., and Sanderson, B. M.: The Scenario Model Intercomparison Project (ScenarioMIP) for CMIP6, Geosci. Model Dev., 9, 3461–3482, https://doi.org/10.5194/gmd-9-3461-2016

Pryor, S. C., Barthelmie, R. J., Bukovsky, M. S., Leung, L. R., & Sakaguchi, K. (2020). Climate change impacts on wind power generation. *Nature Reviews Earth & Environment*, *1*(12), 627–643. https://doi.org/10.1038/s43017-020-0101-7

Rahimi, S., Krantz, W., Lin, Y.-H., Bass, B., Collins, E., Goldenson, N., Hall, A., and Lebo, Z.: 2022. Nine potential futures for the western United States: Dynamically downscaling climate models down to the landscape scale. J. Climate., in preparation.

Reboita Michelle Simões, Amaro, T. R., & de Souza, M. R. (2018). Winds: intensity and power density simulated by regcm4 over south america in present and future climate. *Climate Dynamics : Observational, Theoretical and Computational Research on the Climate System*, *51*(1-2), 187–205. https://doi.org/10.1007/s00382-017-3913-5

Riahi, K., Rao, S., Krey, V., Cho, C., Chirkov, V., Fischer, G., Kindermann, G., Nakicenovic, N., & Rafaj, P. (2011). Rcp 8.5—a scenario of comparatively high greenhouse gas emissions. *Climatic Change : An Interdisciplinary, International Journal Devoted to the Description, Causes and Implications of Climatic Change*, *109*(1-2), 33–57. https://doi.org/10.1007/s10584-011-0149-y

Richter, I., & Tokinaga, H. (2020). An overview of the performance of cmip6 models in the tropical atlantic: mean state, variability, and remote impacts. *Climate Dynamics : Observational, Theoretical and Computational Research on the Climate System*, *55*(9-10), 2579–2601. https://doi.org/10.1007/s00382-020-05409-w

Salamanca, F., Martilli, A., Tewari, M., & Chen, F. (2011). A Study of the Urban Boundary Layer Using Different Urban Parameterizations and High-Resolution Urban Canopy Parameters with WRF, *Journal of Applied Meteorology and Climatology*, *50*(5), 1107-1128. Retrieved May 6, 2022, from https://journals.ametsoc.org/view/journals/apme/50/5/2010jamc2538.1.xml

Sawadogo, W., Reboita, M.S., Faye, A. *et al.* Current and future potential of solar and wind energy over Africa using the RegCM4 CORDEX-CORE ensemble. *Clim Dyn* **57,** 1647–1672 (2021). https://doi.org/10.1007/s00382-020-05377-1

Schaaf, B., Von, S. H., & Feser, F. (2017). Does spectral nudging have an effect on dynamical downscaling applied in small regional model domains? Monthly Weather Review, 145(10), 4303–4311. https://doi.org/10.1175/MWR-D-17-0087.1

Seroka, G., Fredj, E., Kohut, J., Dunk, R., Miles, T., & Glenn, S. (2018). Sea breeze sensitivity to coastal upwelling and synoptic flow using lagrangian methods. Journal of Geophysical Research: Atmospheres, 123(17), 9443–9461. https://doi.org/10.1029/2018JD028940

Skamarock, W. C., Klemp, J. B., Dudhia, J., Gill, D. O., Liu, Z., Berner, J., Wang, W., Powers, J. G., Duda, M. G., Barker, D. M. and Huang, X.-Y. (2019): A Description of the Advanced Research WRF Version 4. NCAR Tech. Note NCAR/TN-556+STR, 145 pp..

Varquez, A.C.G., Nakayoshi, M. & Kanda, M. The Effects of Highly Detailed Urban Roughness Parameters on a Sea-Breeze Numerical Simulation. *Boundary-Layer Meteorol* **154,** 449–469 (2015). https://doi.org/10.1007/s10546-014-9985-4

Veron, D. E., Brodie, J. F., Shirazi, Y. A., & Gilchrist, J. R. (2018). Modeling the electrical grid impact of wind ramp-up forecasting error offshore in the mid-atlantic

region. Journal of Renewable and Sustainable Energy, 10(1), 013308–013308. https://doi.org/10.1063/1.4990684

Vu Dinh, Q., Doan, Q.-V., Ngo-Duc, T., Nguyen Dinh, V., & Dinh Duc, N. (2022). Offshore wind resource in the context of global climate change over a tropical area. *Applied Energy*, *308*. https://doi.org/10.1016/j.apenergy.2021.118369

Wiser, R., Rand, J., Seel, J. *et al.* Expert elicitation survey predicts 37% to 49% declines in wind energy costs by 2050. *Nat Energy* **6,** 555–565 (2021). https://doi.org/10.1038/s41560-021-00810-z

Wu, J., Zha, J., & Zhao, D. (2016). Estimating the impact of the changes in land use and cover on the surface wind speed over the east china plain during the period 1980-2011. *Climate Dynamics : Observational, Theoretical and Computational Research on the Climate System*, *46*(3-4), 847–863. https://doi.org/10.1007/s00382-015-2616-z

Wu, J., Shi, Y., & Xu, Y. (2020). Evaluation and Projection of Surface Wind Speed Over China Based on CMIP6 GCMs. *Journal of Geophysical Research: Atmospheres*, *125*(22). https://doi.org/10.1029/2020JD033611

Xia, G., Draxl, C., Optis, M., & Redfern, S. (2022). Detecting and characterizing simulated sea breezes over the us northeastern coast with implications for offshore wind energy. *Wind Energy Science*, *7*(2), 815–829. https://doi.org/10.5194/wes-7-815-2022

Yan, Z. W., Wang, J., Xia, J. J., & Feng, J. M. (2016). Review of recent studies of the climatic effects of urbanization in China. In *Advances in Climate Change Research* (Vol. 7, Issue 3, pp. 154–168). National Climate Center. https://doi.org/10.1016/j.accre.2016.09.003

Zeng, Z., Ziegler, A. D., Searchinger, T., Yang, L., Chen, A., Ju, K., Piao, S., Li, L. Z. X., Ciais, P., Chen, D., Liu, J., Azorin-Molina, C., Chappell, A., Medvigy, D., & Wood, E. F. (2019). A reversal in global terrestrial stilling and its implications for wind energy production. *Nature Climate Change*, *9*(12), 979–985. https://doi.org/10.1038/s41558-019-0622-6

Zhang, Z., Wang, K., Chen, D., Li, J., & Dickinson, R. (2019). Increase in surface friction dominates the observed surface wind speed decline during 1973-2014 in the northern hemisphere lands. *Journal of Climate*, *32*(21), 7421–7435. https://doi.org/10.1175/JCLI-D-18-0691.1

Zhao, L., Oleson, K., Bou-Zeid, E., Krayenhoff, E. S., Bray, A., Zhu, Q., Zheng, Z., Chen, C., & Oppenheimer, M. (2021). Global multi-model projections of local urban climates. *Nature Climate Change*, *11*(2), 152–157. https://doi.org/10.1038/s41558-020-00958-8

Zhou, Y., Guan, H., Huang, C., Fan, L., Gharib, S., Batelaan, O., & Simmons, C. (2019). Sea breeze cooling capacity and its influencing factors in a coastal city. *Building and Environment*, *166*. https://doi.org/10.1016/j.buildenv.2019.106408

Appendix A

OFFSHORE WIND SPEED DISTRIBUTIONS

The distribution of annual offshore wind speeds at 120-m shifts slightly towards faster wind speeds as a result of urbanization (SSP5_HIST – HIST_HIST) and more substantially due to climate change (HIST_RCP8.5 – HIST_HIST) (Fig. 8a,b). On summer days, both urbanization and climate change have substantially larger impacts on the shift towards more frequent higher wind speeds, although climate change impacts are larger during this time frame as well (Fig 9a,b).

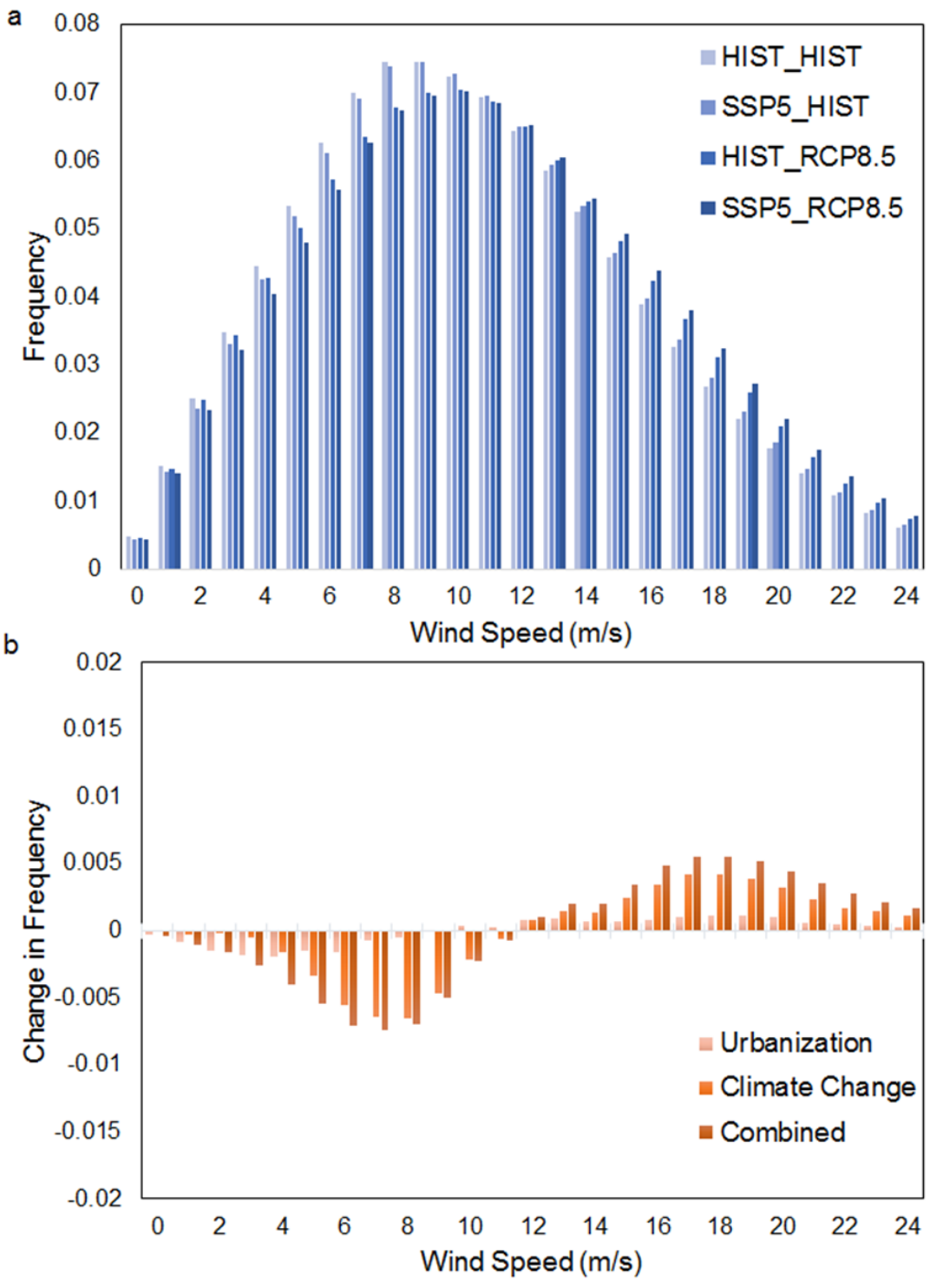
a
0.08
0.07
0.06
0.05
0.04
0.03
0.02
0.01
0
Frequency
HIST_HIST
SSP5_HIST
HIST_RCP8.5
SSP5_RCP8.5
0 2 4 6 8 10 12 14 16 18 20 22 24
Wind Speed (m/s)
b
0.02
0.015
0.01
0.005
0
-0.005
-0.01
-0.015
-0.02
Change in Frequency
Urbanization
Climate Change
Combined
0 2 4 6 8 10 12 14 16 18 20 22 24
Wind Speed (m/s)

Figure 8: (a) Annual average 120-m offshore wind speed distribution for each scenario and (b) changes to that distribution due to urbanization (SSP5_HIST – HIST_HIST), climate change (HIST_RCP8.5 – HIST_HIST), and their combined effects (SSP5_RCP8.5 – HIST_HIST).

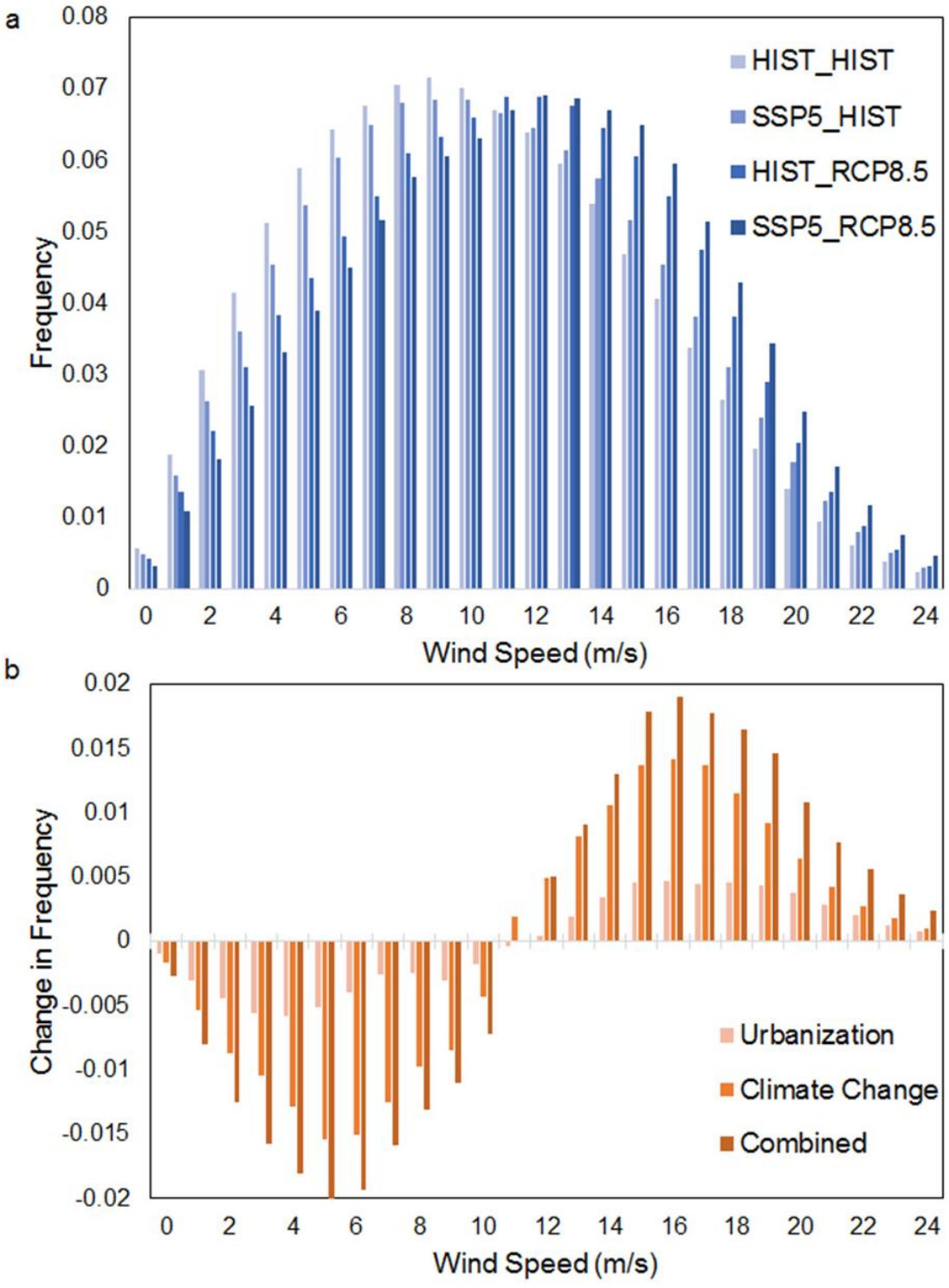
a
0.08
0.07
0.06
0.05
0.04
0.03
0.02
0.01
0
Frequency
HIST_HIST
SSP5_HIST
HIST_RCP8.5
SSP5_RCP8.5
0 2 4 6 8 10 12 14 16 18 20 22 24
Wind Speed (m/s)
b
0.02
0.015
0.01
0.005
0
-0.005
-0.01
-0.015
-0.02
Change in Frequency
Urbanization
Climate Change
Combined
0 2 4 6 8 10 12 14 16 18 20 22 24
Wind Speed (m/s)

Figure 9: (a) Summer daytime (8am – 8pm) 120-m offshore wind speed distribution for each scenario and (b) changes to that distribution due to urbanization (SSP5_HIST – HIST_HIST), climate change (HIST_RCP8.5 – HIST_HIST), and their combined effects (SSP5_RCP8.5 – HIST_HIST).

Appendix B

ANNUAL IMPACTS ON WIND SPEED

Climate change causes increasing annual average 120-m wind speeds throughout the coastal Mid-Atlantic and similar to summertime impacts, the largest changes are found offshore (Fig. 10b). Urbanization causes slight increases in 120-m wind speed offshore (<0.2 m/s) and decreasing wind speed over land (Fig. 10a). At 10-m above the surface, climate change shows minimal impacts on annual wind speeds (Fig. 10e) while urbanization causes substantial wind speed decreases over urbanizing areas (0.6 - 1.2 m/s, Fig. 10d).

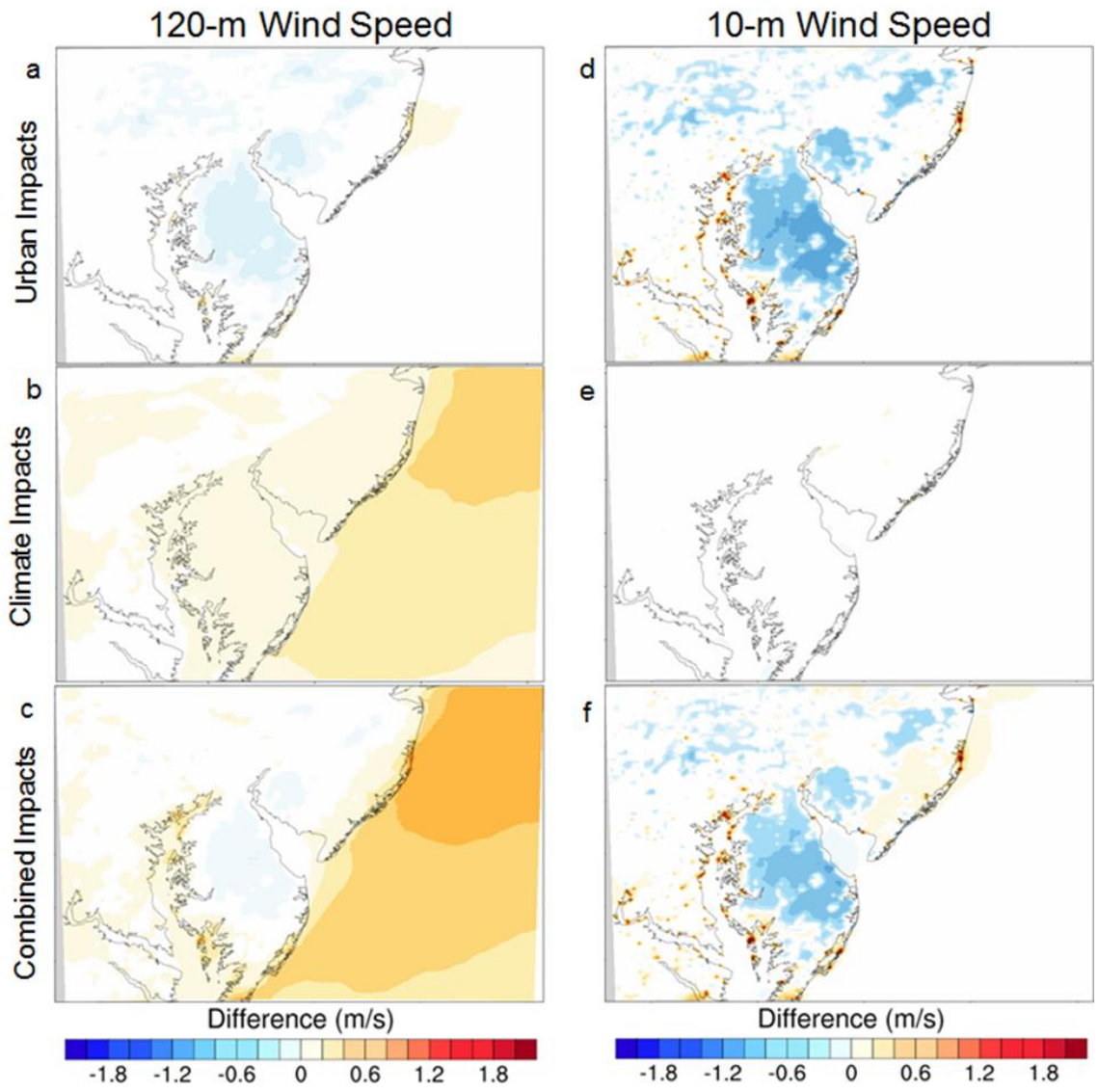

Figure 10: Urbanization (SSP5_HIST – HIST_HIST), climate change (HIST_RCP8.5 – HIST_HIST), and combined (SSP5_RCP8.5 – HIST_HIST) impacts on annual average (a, b, c) 120-m and (d, e, f) 10-m wind speed.

Appendix C

ANNUAL IMPACTS ON TEMPERATURE AND DEW POINT TEMPERATURE

Urbanization causes annual average surface temperatures to increase by 1 - 2.5 ℃ (Fig. 11a) as a result of the urban heat island effect and causes surface dew point temperatures to decrease by 0.5 - 2.0 ℃ (Fig. 11d) by removing the moisture released by vegetation. Climate change causes substantial increases in both temperature (3.0 - 6.0 ℃, Fig. 11b) and dew point temperature (3.5 - 6.5 ℃, Fig. 11e). Temperature increases are amplified in the combined scenario (SSP5_RCP8.5, 11c) while drying surface conditions as a result of urbanization mitigate the increasing dew point temperatures due to climate change in the combined scenario (Fig. 11f).

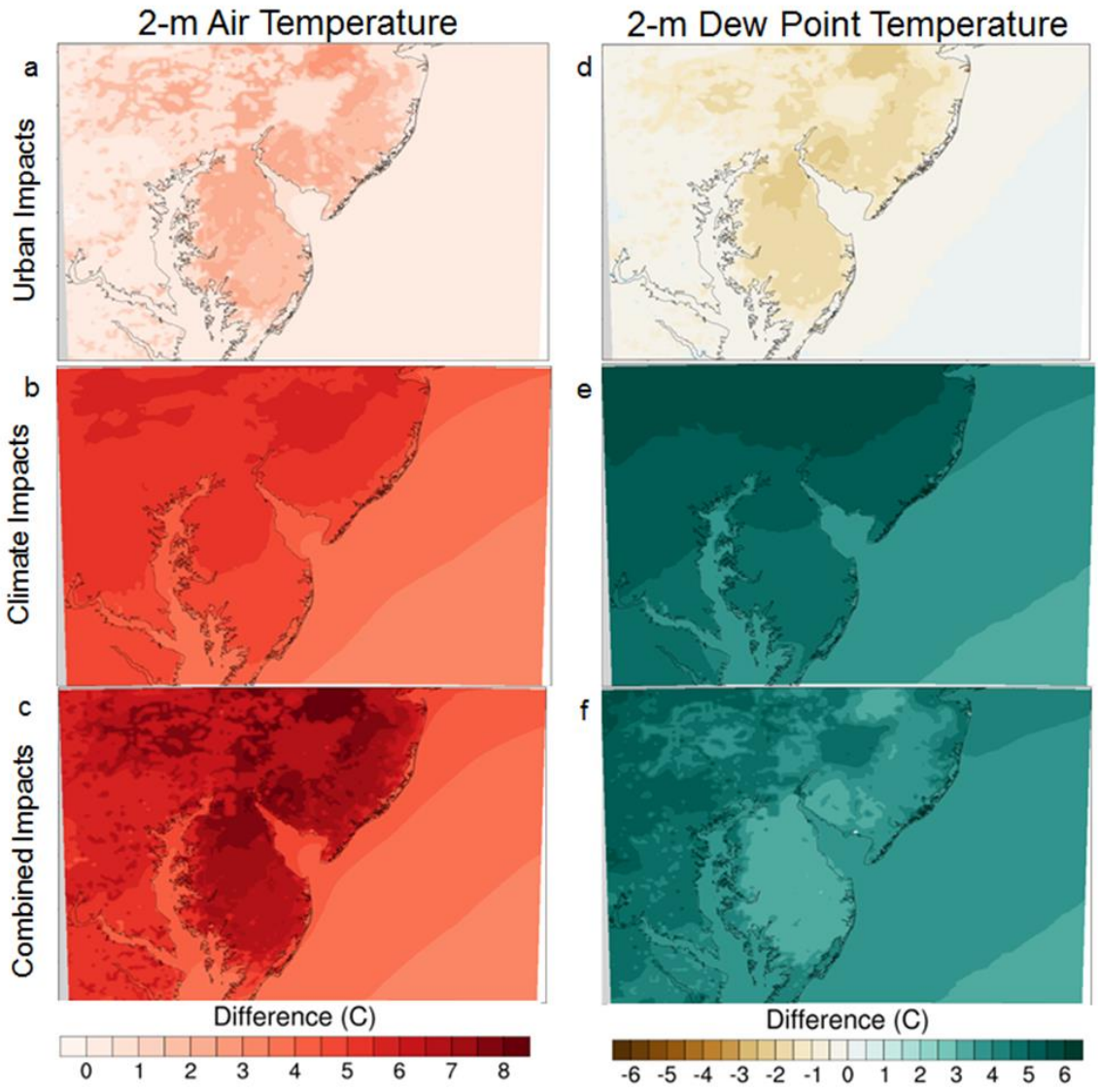

Figure 11: Urbanization (SSP5_HIST – HIST_HIST), climate change (HIST_RCP8.5 – HIST_HIST), and combined (SSP5_RCP8.5 – HIST_HIST) impacts on annual average (a, b, c) 2-m temperature and (d, e, f) 2-m dew point temperature.

Appendix D

ANNUAL IMPACTS ON SEA LEVEL PRESSURE AND PLANETARY BOUNDARY LAYER HEIGHT

Urbanization causes slight decreases in annual average sea level pressure centered over coastal New Jersey and Delaware (Fig. 12a), which creates a marginally stronger coastal pressure gradient. Climate change causes larger increases in the coastal pressure gradient (Fig. 12b) as a result of decreasing pressure over land and increasing pressure over the ocean. Combined urbanization and climate change forcing causes the largest increases in the coastal pressure gradient (Fig. 12c). While climate change causes slight decreases in PBLH over the ocean (50 - 100 m, Fig. 12e), urbanization causes larger increases in PBLH over urbanizing areas (100 - 250 m, Fig. 12d) likely due to increased surface roughness.

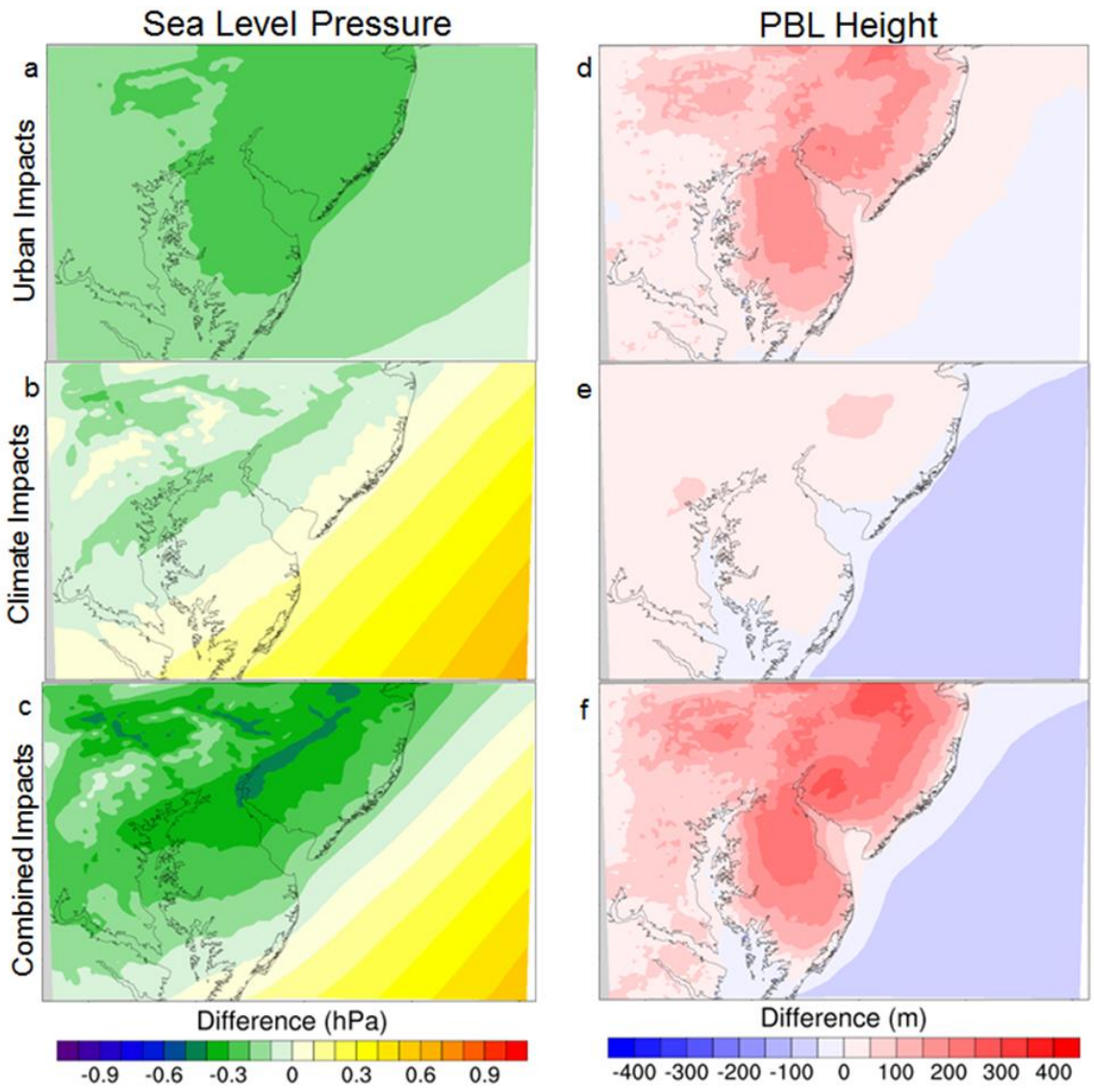

Figure 12: Urbanization (SSP5_HIST – HIST_HIST), climate change (HIST_RCP8.5 – HIST_HIST), and combined (SSP5_RCP8.5 – HIST_HIST) impacts on annual average (a, b, c) sea level pressure and (d, e, f) planetary boundary layer (PBL) height.

Appendix E

ANNUAL AVERAGE INTERACTION BETWEEN CLIMATE CHANGE AND URBANIZATION

Annual average interaction between climate change and urbanization ((SSP5_RCP8.5 – HIST_RCP8.5) – (SSP5_HIST – HIST_HIST)) is minimal for 120-m wind speed and MSLP (<0.1 m/s, hPa) (Fig. 13a,b). Similar to interaction effects on extreme heat conditions in the summer, annual average 2-m temperature interaction effects are mostly positive and larger than other variables. The largest positive interaction between climate change and urbanization on 2-m temperature is in southern New Jersey (0.2 – 0.6 ℃) (Fig. 13c).

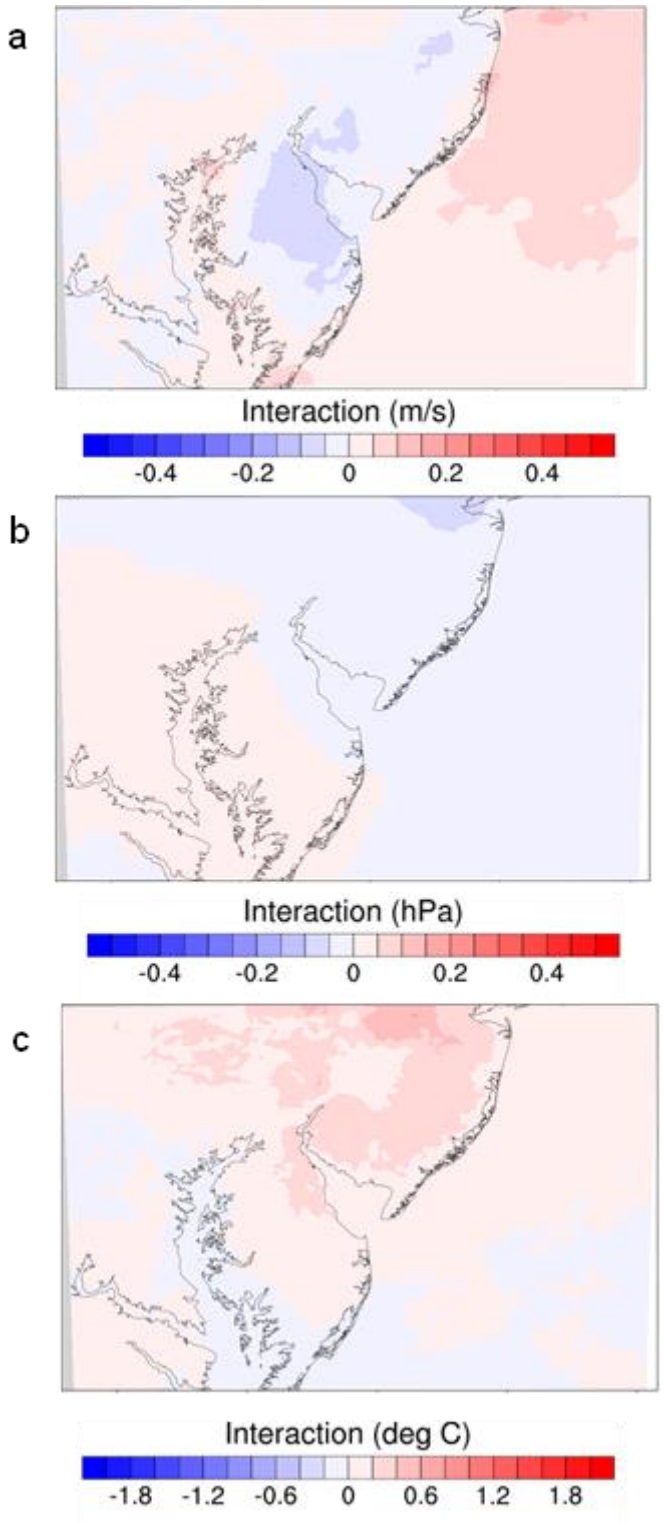
a
Interaction (m/s)
-0.4
-0.2
0
0.2
0.4
b
Interaction (hPa)
-0.4
-0.2
0
0.2
0.4
c
Interaction (deg C)
-1.8
-1.2
-0.6
0
0.6
1.2
1.8

Figure 13: Interaction effects ((SSP5_RCP8.5 – HIST_RCP8.5) – (SSP_HIST – HIST_HIST) on annual average (a) 120-m wind speed, (b) mean sea level pressure (MSLP), and (c) 2-m temperature.